Solid Primary Retroperitoneal Masses in Adults: An Imaging Approach

Vaibhav Gulati[1] M. Sarthak Swarup[1] Jyoti Kumar[1]

[1] Maulana Azad Medical College and Associated Lok Nayak Hospital, New Delhi, India

Indian J Radiol Imaging 2022;32:235–252.

Address for correspondence Dr. Jyoti Kumar, MD, Professor, Department of Radio-diagnosis, Maulana Azad Medical College, New Delhi, India (e-mail: drjyotikumar@gmail.com).

Abstract

Mass lesions in the retroperitoneal space may be primary or secondary. Primary retroperitoneal mass lesions are relatively uncommon as compared to pathology that arises secondarily from retroperitoneal organs. These may be solid or cystic lesions. The overlapping imaging features of various solid primary retroperitoneal tumors make the diagnosis difficult, and hence, histopathology remains the mainstay of diagnosis. This paper provides a brief review of the anatomy of the retroperitoneal space and provides an algorithmic approach based on cross-sectional imaging techniques to narrow down the differential diagnosis of solid primary retroperitoneal masses encountered in the adult population.

Keywords
- Retroperitoneal space
- Anatomy
- Imaging
- Solid
- Algorithmic approach

Introduction

Primary retroperitoneal masses are a rare but heterogeneous group of lesions that arise within the retroperitoneal space but outside the major retroperitoneal organs like kidneys, adrenal, pancreas, duodenum, and colon. They comprise various neoplastic and non-neoplastic masses and can be categorized into solid or cystic based upon their imaging appearance.

Retroperitoneal masses are often asymptomatic, and their presentation is nonspecific, depending upon the extent, size, and invasion of surrounding structures. Cross-sectional imaging with computed tomography (CT) or magnetic resonance imaging (MRI) is the backbone of non-invasive characterization of retroperitoneal masses. CT provides better spatial resolution and is the best modality to detect calcifications. MRI provides better soft-tissue contrast and is more often used as a problem-solving tool. Ultrasonography plays a rather limited role but can be used to assess vascularity and vascular invasion.[1] Confirmation of diagnosis often requires histopathological assessment owing to the overlapping characteristics of the lesions on imaging. Ultrasonography and CT guidance also enable the safe procurement of samples for histological analysis.[2]

This article aims to provide a brief review of the normal retroperitoneal anatomy, an overview of the cross-sectional imaging features of the common primary solid retroperitoneal mass lesions in adults, and a diagnostic algorithmic approach to assist radiologists in narrowing the differential diagnosis. A wide variety of solid primary retroperitoneal mass lesions are encountered exclusively or predominantly in the pediatric population. These include neuroblastoma, ganglioneuroblastoma, teratoma, rhabdomyosarcoma, and hemangioma. The detailed description of their imaging appearances is out of the scope of this article.

Anatomy of the Retroperitoneal Space

The retroperitoneal space extends from the diaphragm superiorly to the pelvis inferiorly and is limited by the transversalis fascia posteriorly and by the parietal peritoneum anteriorly. The retroperitoneal space is divided by various fasciae into three primary compartments—the anterior

published online
July 13, 2022

DOI https://doi.org/10.1055/s-0042-1744142.
ISSN 0971-3026.

Thieme Medical and Scientific Publishers Pvt. Ltd., A-12, 2nd Floor, Sector 2, Noida-201301 UP, India

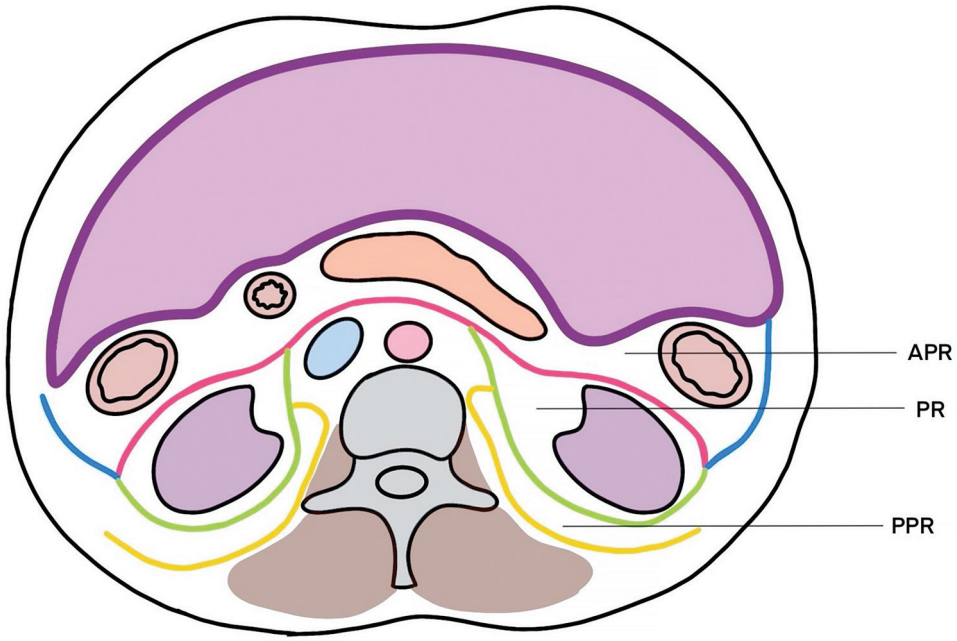

Fig. 1 Cross-sectional diagram of the abdomen depicting the retroperitoneal compartments: APR, anterior pararenal space; PPR, posterior pararenal space; PR, perirenal space. Green—posterior renal fascia. Pink—anterior renal fascia. Yellow—transversalis fascia. Blue—lateroconal fascia.

pararenal (APR), posterior pararenal (PPR), and perirenal (PR) space, in addition to one, central, great vessel compartments (►**Fig. 1**).[2,3]

The PR space mainly contains structures of the genitourinary system—the kidneys along with the adrenal glands, the ureters, their vasculature, and lymphatics. It is shaped like an inverted cone pointing toward the pelvis and limited by the anterior renal fascia (Gerota's fascia) anteriorly and the posterior renal fascia (Zuckerkandl's fascia) posteriorly. It is enclosed inferiorly as the anterior and posterior renal fasciae fuse to form the combined interfascial plane. The APR space is home to parts of the ascending and descending colon, the duodenum, and the pancreas. It is limited by the parietal peritoneum anteriorly, posteriorly by the anterior renal fascia, and laterally by the lateroconal fascia. The PPR is a potential space containing only fat and is bounded anteriorly by the posterior renal fascia and posteriorly by the transversalis fascia, which lines the psoas major and quadratus lumborum muscles. The central compartment is located between the PR spaces, posterior to the APR space, and anterior to the spine extending from T12 to L4-L5 vertebrae. It houses the abdominal aorta along with its branches, the inferior vena cava (IVC) and its tributaries, lymphatic chains, and the abdominal sympathetic trunk. Superiorly, the right side of the retroperitoneal space is continuous with the bare area of the liver, whereas the left side extends up to the diaphragm.[3]

The concept of interfascial planes has now become integral in explaining the anatomy and pathology of the retroperitoneum. This advocates that the fasciae described above are not just "walls" that divide the retroperitoneal space but are layered planes with potential spaces within them, which can act as channels for the spread of disease beyond the compartment of origin.[4] The retromesentric plane develops from the multiple layers that make up Gerota's fascia. Similarly, the lateroconal plane corresponds to the lateroconal fascia and the retrorenal plane to the Zuckerkandl's fascia. These three fascial planes unite at a point known as the fascial trifurcation where the anterior and posterior fascial planes meet and continue downward as the combined interfascial plane as mentioned above.[4] On CT and MRI, retroperitoneal fascial planes are usually detected when there is an abundance of retroperitoneal fat. Fascia measuring greater than 3 mm is considered thickened and fascial thickening is a sensitive, although nonspecific sign of a retroperitoneal pathologic process.[5]

Mass Localization

Accurate diagnosis of primary retroperitoneal tumors is often challenging for radiologists. After ascertaining the origin of the lesion from the retroperitoneum with the aid of various signs described below and illustrated in ►**Figs. 2** to **4**, the characterization of lesions is done based on solid/cystic nature, pattern of spread, vascularity, and specific lesion components like fat, myxoid stroma, calcification, hemorrhage, and enhancement pattern.[5,6]

Labeling a lesion as a primary retroperitoneal mass requires confirmation of its location within the retroperitoneal space as well as the exclusion of the possibility of its origin from a retroperitoneal organ. Anterior displacement of the normal retroperitoneal organs (kidneys, adrenal glands, ureters, ascending and descending colon, pancreas, and portions of the duodenum), as well as retroperitoneal major vasculature and their branches, strongly suggests that the lesion arises from or is localized to the retroperitoneum. The

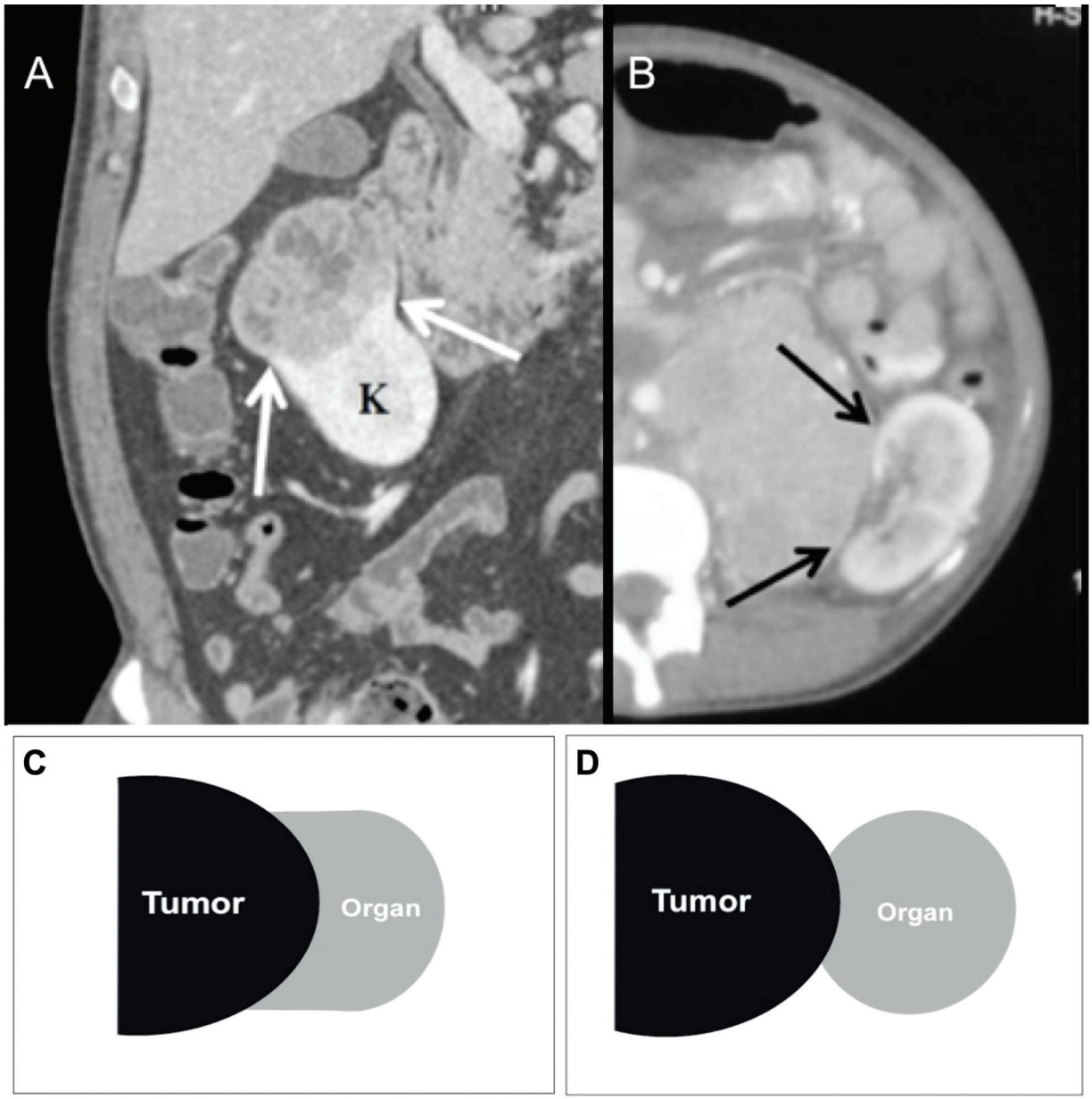

Fig. 2 (**A**) Coronal contrast-enhanced CT image of a 45-year-old male shows a heterogeneously enhancing mass lesion with positive beak/claw sign (*arrows*) along its contact surface with the right kidney (K) in a case of renal cell carcinoma. (**B**) Axial contrast-enhanced CT image in an 18-year-old female reveals heterogeneously enhancing mass that demonstrates negative beak sign (*arrows*) in relation to the left kidney. This indicates a primary retro-peritoneal origin of the mass. Schematic diagrams illustrating (**C**) the positive "beak" sign and (**D**) negative "beak" sign.

following signs aid in determining the primary retroperitoneal origin of a mass.[7,8]

- *Beak or claw sign*—When a mass lesion creates an acute angle or a "beak"-like shape at the edge of an organ it abuts, it is suggestive of the lesion originating from that organ. If a mass creates obtuse angles and dull edges as it compresses an organ, it suggests that it does not originate from that organ (►**Fig. 2**). Hence, a negative beak sign points to a primary retroperitoneal mass.
- *Embedded organ sign*—A mass lesion will deform a hollow viscus or malleable organ and make it assume a crescentic shape if it does not originate from it (negative embedded organ sign). Masses that originate from an organ encase it and the organ appears to be "embedded" within (►**Fig. 3**).
- *Invisible or phantom organ sign*—Large masses that originate from small-sized organs make the native organ hard to visualize on imaging, which then becomes "invisible," for example, a large adrenal mass that makes the adrenal gland "invisible" (►**Fig. 4**).
- *Prominent feeding artery sign*—Hypervascular masses may sometimes have a large feeding vessel that can be visualized on MRI or CT which can help in identifying the organ of origin. For example, a mass deriving its supply from the renal artery indicates renal origin.

Solid retroperitoneal neoplastic lesions have been classified according to the tissue of origin and broadly include

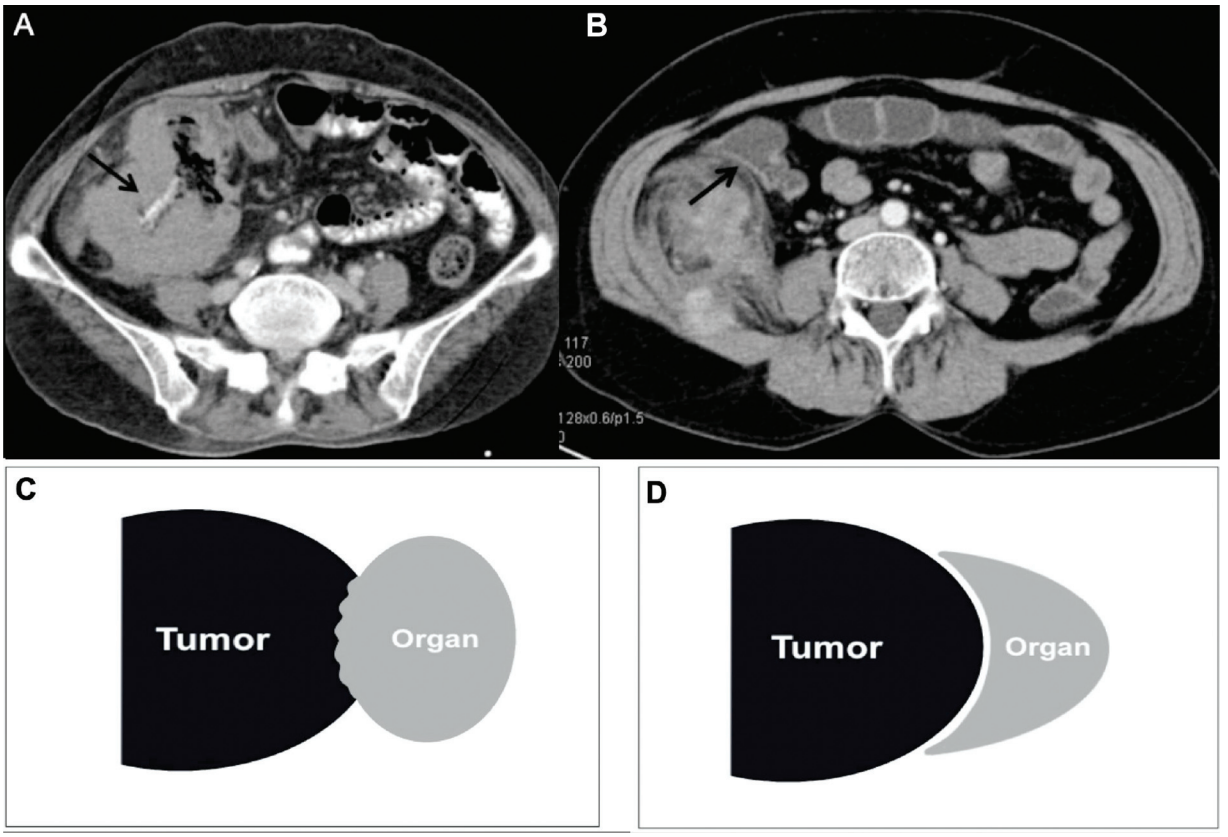

Fig. 3 (**A**) Post-contrast axial CT image of a 55-year-old female with colon carcinoma demonstrates a heterogeneously enhancing retroperitoneal mass involving the right colon which is embedded within the mass (*arrow*), illustrating the positive embedded organ sign. (**B**) Post-contrast axial CT image in a 50-year-old female with primary retroperitoneal sarcoma shows a right-sided heterogenous infiltrative mass in the retroperitoneum with involvement of the adjacent posterior abdominal wall muscles. The mass displaces and deforms the ascending colon (*arrow*) illustrating the negative embedded organ sign. Schematic diagrams illustrating the (**C**) positive "embedded organ" sign and (**D**) negative "embedded organ" sign.

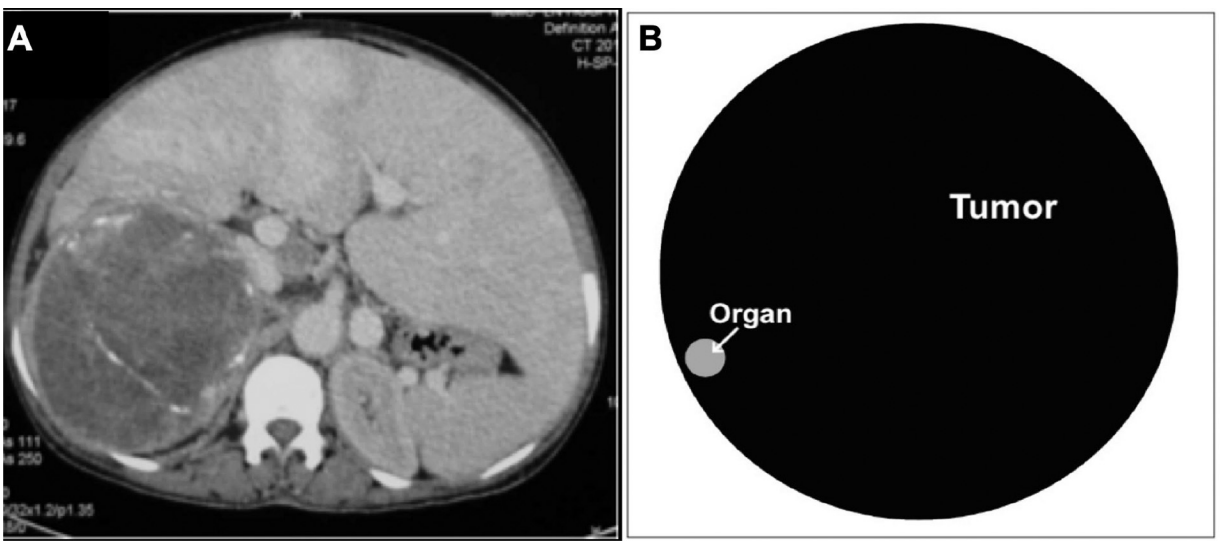

Fig. 4 (**A**) Contrast-enhanced axial CT image of a 35-year-old female with retroperitoneal pheochromocytoma shows a large heterogeneous mass in the right suprarenal location immediately behind the IVC displacing it anteriorly, with an undetectable right adrenal gland illustrating the "phantom organ" sign. (**B**) Schematic diagram illustrating the "phantom organ" sign.

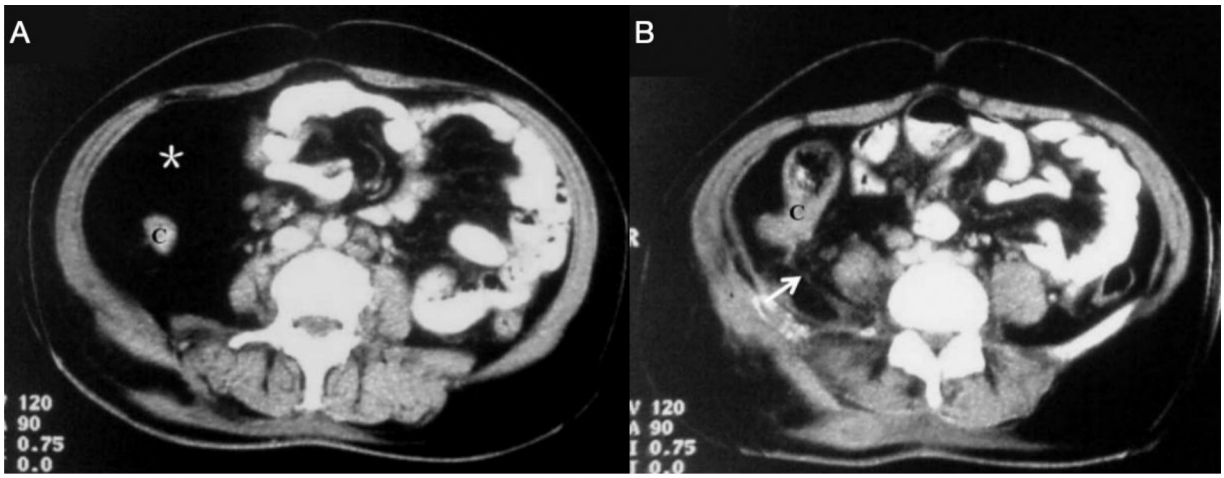

Fig. 5 Retroperitoneal well-differentiated liposarcoma in a 35-year-old woman. (**A, B**) Axial contrast-enhanced CT images demonstrate a large, illdefined, fatty mass lesion (*asterisk*) involving the right anterior pararenal space surrounding and anteriorly displacing the ascending colon (**C**). There is medial displacement of small bowel loops and mesentery. Note the subtle soft-tissue septations and nodularity within the mass (*arrow*).

mesenchymal tumors/sarcomas, lymphoid tumors, neurogenic tumors, and germ cell tumors (►**Table 1**).[3,6] Common primary solid non-neoplastic entities of the retroperitoneum include retroperitoneal fibrosis (RPF), non-Langerhans histiocytosis (Erdheim–Chester disease [ECD]), and extramedullary hematopoiesis (EMH).

Mesenchymal Tumors

Most of the primary retroperitoneal neoplasms are of mesenchymal origin, with sarcomas constituting about 47 to 57% of these.[9] Liposarcomas (LS), leiomyosarcomas, and malignant fibrous histiocytomas together account for more than 80% of these tumors.[1,7] Sarcomas are usually seen in the elderly and are often large at presentation.[10] Most sarcomas have a pseudocapsule that represents compressed surrounding normal tissue.[7] Surgical resection is the definitive treatment for retroperitoneal sarcomas.[10,11] In general, extensive vascular involvement, peritoneal implants, and distant metastatic disease suggest unresectable disease.[5] Recurrence rates are high in all types of sarcomas, independent of histological grade.[7]

Table 1 Classification of common solid retroperitoneal neoplastic mass lesions according to the tissue of origin

Tissue of origin	Benign pathologies	Malignant pathologies
1. *Mesodermal neoplasms*		
Fat tissue	Lipoma	Liposarcoma
Connective tissue	Fibroma	Malignant fibrous histiocytoma/ undifferentiated pleomorphic sarcoma, and fibrosarcoma
Smooth muscle	Leiomyoma	Leiomyosarcoma
2. *Lymphoid neoplasms*		
Lymphoid tissue		Lymphoma
3. *Neurogenic neoplasms*		
Ganglion cell	Ganglioneuroma	Ganglioneuroblastoma and neuroblastoma
Paraganglionic system	Paraganglioma or Pheochromocytoma	Malignant paraganglioma or pheochromocytoma
Nerve sheath	Schwannoma, neurofibroma	Malignant nerve sheath tumors
4. *Germ cell neoplasms*		
Embryonic tissue	Teratoma (mature and immature)	Teratoma (malignant) and primary extragonodal germ cell tumor (seminomatous and non-seminomatous)

Liposarcoma

Liposarcoma (LS) is the most common type of retroperitoneal sarcoma and accounts for 40% of all retroperitoneal sarcomas.[5,11] LS generally occurs in the fifth to seventh decades of life and does not have any gender predilection.[12] It tends to grow to large sizes (up to 20 cm) before coming to clinical attention as patients only present with symptoms of mass effect. Histopathologically, it can be classified into well-differentiated, myxoid, de-differentiated, and pleomorphic types.[13] Different histological subtypes may coexist, and the most aggressive component is then used to classify the lesion. LS is relatively easy to identify on imaging, especially the well-differentiated forms, owing to the presence of a large amount of fat.[7]

A well-differentiated LS, the most common subtype, is seen as a well-defined lobular lesion with smooth margins on CT with macroscopic fat comprising >75% of the tumor (►**Fig. 5**). It tends to have internal septations and nodularity with mild-to-moderate contrast enhancement.[14] It may be confused with a lipoma, but lipomas are exceedingly rare in the retroperitoneum. Moreover, lesion size >10 cm, presence of nodular or globular enhancing soft-tissue components, and thickened septae (>3 mm) favor a diagnosis of LS over lipoma.[5,15] MRI shows high signal intensity on T1- and intermediate signal intensity on T2-weighted images with the loss of signal on fat-suppressed images corresponding to areas of fat.

Myxoid LS is the second most common subtype and tends to occur in a slightly younger age group. It is seen as a lobular, heterogeneous lesion and the myxoid component is typically hypodense to muscle on CT (►**Fig. 6**). On non-contrast CT and MRI, it typically shows a "pseudocystic" appearance due to water attenuation/intensity myxoid stroma.[14] Sometimes it characteristically shows a gradual and heterogeneous pattern of internal enhancement on delayed post-contrast images, unlike true cystic lesions.[5,7] A potential pitfall is that the fatty component at the margin of the mass may simulate extraperitoneal fat and be missed.[5,16]

A de-differentiated LS usually contains a well-differentiated lipogenic component and a dedifferentiated non-lipogenic component (►**Fig. 7**). About 20% of the lesions may not have any identifiable fat and may be difficult to diagnose on imaging.[7] Calcification is seen in approximately 30% of cases.[7]

Pleomorphic LS is the least common and is seen as a heterogeneous soft-tissue mass with or without necrosis and contains little or no macroscopic fat, often indistinguishable from other malignant soft-tissue masses.[2] It is an aggressive tumor with a tendency for early lung metastasis.

The treatment of choice, wherever feasible, is surgical resection with wide negative margins. However, recurrence remains very common and occurs in up to 50% of well-differentiated forms and in up to 80% of dedifferentiated forms.[12,17]

Liposarcoma
- Well-defined lobular mass is observed with the macroscopic fatty component.
- Well-differentiated form is characterized by a large amount of fat, often with internal septations and nodularity.
- Myxoid forms show characteristic "pseudocystic" appearance on non-contrast CT and MRI.
- Dedifferentiated form has a large non-lipogenic component.
- Pleomorphic liposarcoma (least common form) has little/no macroscopic fat and is indistinguishable from other malignant soft-tissue masses.

Leiomyosarcoma

Leiomyosarcoma is the second most common retroperitoneal sarcoma and represents almost 30% of all retroperitoneal sarcomas.[5,7] It tends to occur more in females and is usually seen in the fifth and sixth decades of life. It arises from smooth muscle tissue in various retroperitoneal structures. Most lesions are extravascular (66%), but mixed (33%) and completely intravascular (5%) masses are also encountered.[1,7] It is the most common primary tumor of the IVC.[5] Patients usually present late when the tumor has grown to large sizes (>10 cm) with symptoms due to mass effect. Metastases to the liver, lymph nodes, and lungs can occur later with progression.[1]

On CT, the lesion is usually well-circumscribed and isoattenuating to muscle with heterogeneous post-contrast

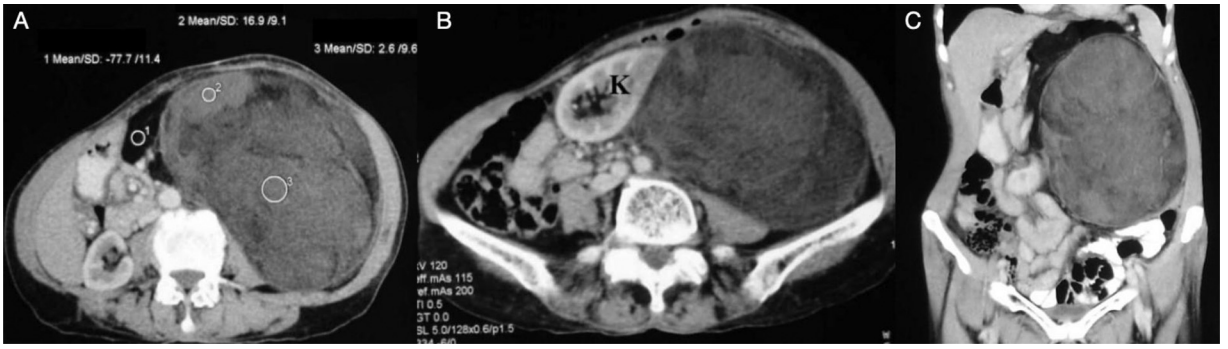

Fig. 6 Retroperitoneal myxoid liposarcoma in a 60-year-old female with a palpable abdominal mass. (**A, B**) Axial and (**C**) coronal contrast-enhanced CT images show a large well-circumscribed heterogeneous left retroperitoneal mass displacing the left kidney (K) anteromedially, spleen superiorly, and bowel loops infero-medially. The lesion shows variable CT attenuation areas related to the presence of macroscopic fat (ROI 1), soft-tissue density component (ROI 2), and low attenuation myxoid (ROI 3) dominant component. Fat in the margin of the mass may simulate extraperitoneal fat and be missed.

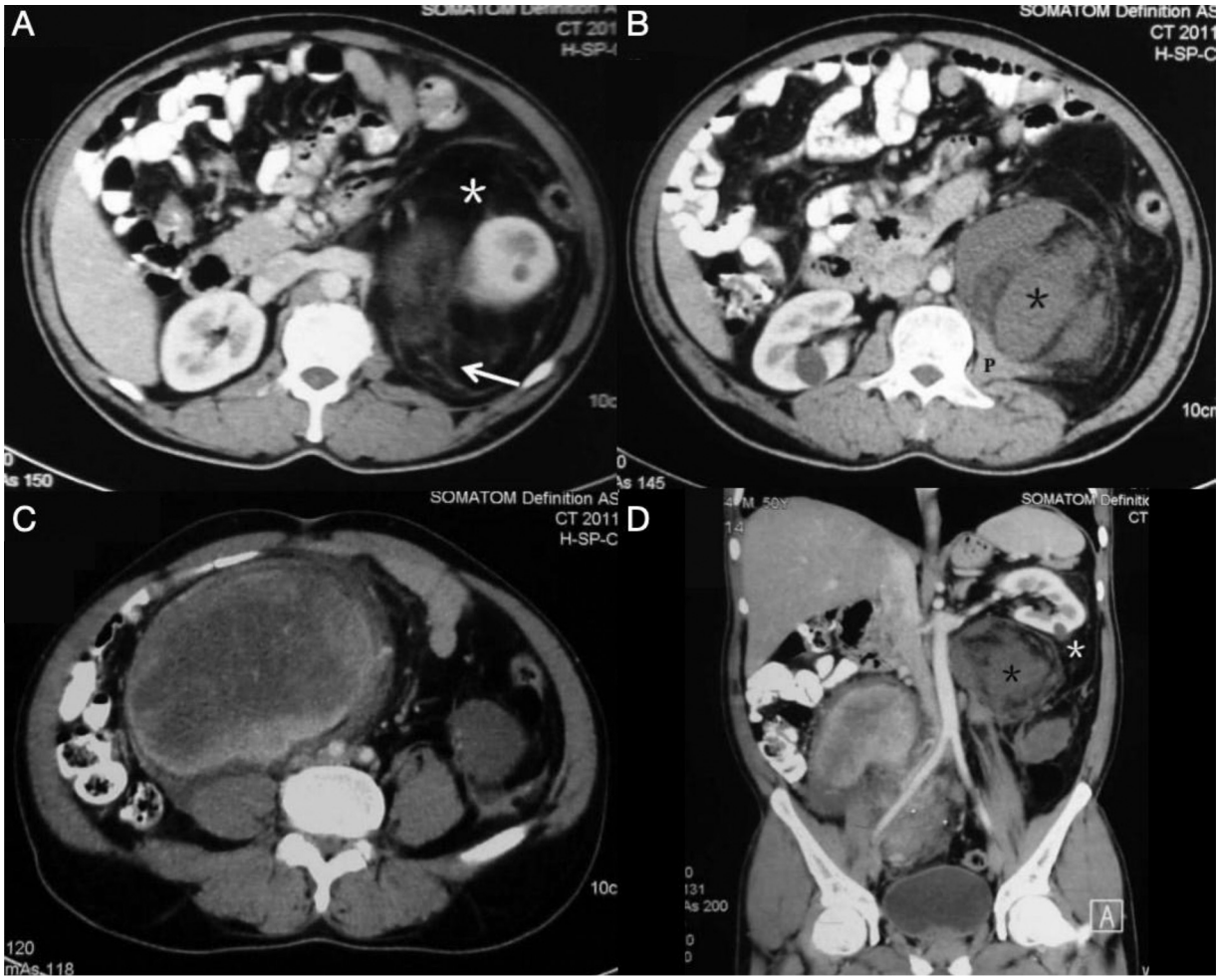

Fig. 7 Retroperitoneal liposarcoma in a 50-year-old man. (**A, B, C**) Axial and (**D**) coronal postcontrast CT images show a large heterogeneously enhancing left-sided retroperitoneal mass with a well-differentiated fatty component (*white asterisk*) superiorly in the perinephric region with linear septations within (*arrow*) and dedifferentiated mass-like areas of soft tissue (*black asterisk*) inferiorly. There is involvement of left psoas muscle (P) with mass-effect and displacement of the left kidney. Distinct, large, heterogeneously enhancing necrotic soft-tissue mass on the right, likely metastasis.

enhancement (►**Fig. 8**). Small lesions may be homogeneous, but large masses are often heterogeneous owing to areas of necrosis and hemorrhage. Internal areas of low attenuation represent necrosis and cystic degeneration, which are common and more extensive than in undifferentiated pleomorphic sarcoma.[7] Calcification and intralesional fat are classically not seen.[5,18] The appearance on MRI varies, having low-to-intermediate signal intensity on T1-weighted and intermediate to high signal intensity on T2-weighted images.[1,7] The necrotic component shows a low-intensity signal on T1- and hyperintense signal on T2-weighted images. Mixed signal intensity and fluid debris levels may be seen in hemorrhagic lesions.[1] The presence of extensive necrosis and involvement of vessel (IVC) help to differentiate leiomyosarcoma from other entities.

Leiomyosarcoma
- Well-circumscribed mass is observed with areas of necrosis and hemorrhage with the involvement of a contiguous vessel.
- Fat and calcification are typically absent.

Undifferentiated Pleomorphic Sarcoma

Undifferentiated pleomorphic sarcoma, previously known as malignant fibrous histiocytoma, is the third most frequently encountered retroperitoneal sarcoma and accounts for 15% of all cases.[7,19] It is also the most common soft-tissue sarcoma in the body and is more common in males, usually occurring in the fifth and sixth decades of life.[1]

Imaging findings are nonspecific, and the lesion is seen as a large, relatively well-circumscribed heterogeneously enhancing soft-tissue mass with or without invasion of adjacent organs (►**Fig. 9**). Areas of necrosis and hemorrhage may be seen, as in leiomyosarcomas, but they are much less extensive here. Calcification, which may be in a ring-like pattern near the periphery or a speckled pattern centrally, is seen in 7 to 20% of cases and, when present, helps to differentiate it from a leiomyosarcoma.[1,2] On MRI, the lesion is seen to have an intermediate T1- and heterogeneously increased T2- signal intensity compared to muscle with well-defined margins.[7] The admixture of solid, cystic, necrotic, hemorrhagic, myxoid, fibrotic, and calcified areas of the lesion can lead to a mosaic of mixed low, intermediate,

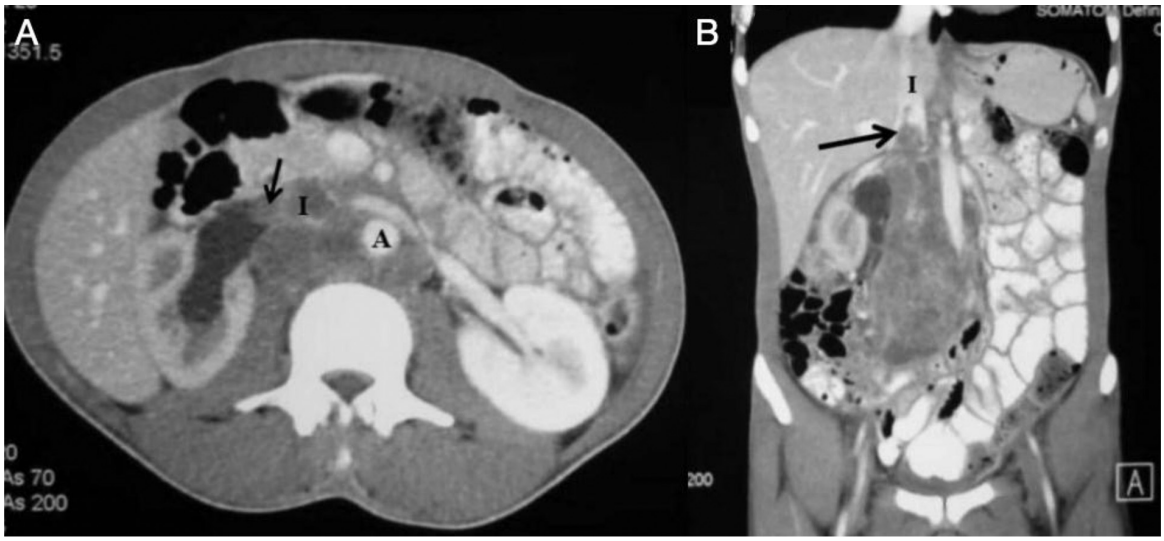

Fig. 8 Retroperitoneal IVC leiomyosarcoma in a 28-year-old male with abdominal pain. (**A**) Contrast-enhanced axial and (**B**) coronal CT images demonstrate a relatively well-circumscribed heterogeneously enhancing mass in the retroperitoneum with extensive necrosis. There is expansion of the IVC (I) with both extraluminal and intraluminal components. There is involvement of both suprarenal and infrarenal segments of the IVC with cranial extension of tumor into the intrahepatic IVC (*large arrow*). The tumor thrombus extends into the right renal vein (*small arrow*) causing mild right-sided hydronephrosis.

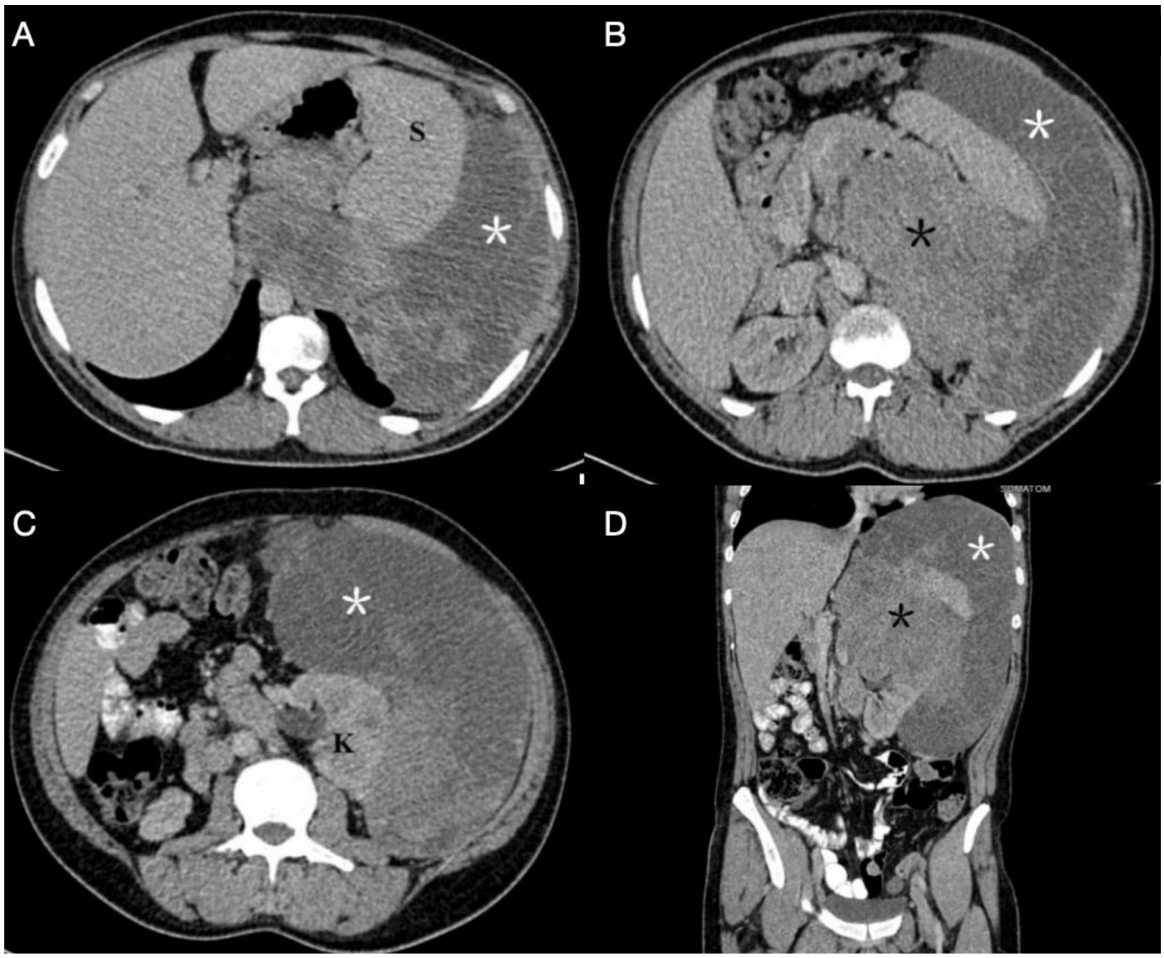

Fig. 9 Contrast-enhanced CT (**A, B, C**) axial and (**D**) coronal images in a 34-year-old male with a palpable mass show a large, circumscribed mass in left retroperitoneum encasing the left kidney (K) with negative beak sign along with anterior displacement of the spleen (S). The lesion is heterogeneous with areas of solid soft tissue (*black asterisk*) and cystic and myxoid components (*white asterisk*). In the absence of fat, myxoid variety of liposarcoma and undifferentiated pleomorphic sarcoma (MFH) appear similar and cannot be differentiated on imaging alone. This was undifferentiated pleomorphic sarcoma.

and high signal intensities on T2-weighted MRI giving rise to the "bowl of fruit" sign.[20]

Undifferentiated pleomorphic sarcoma
- Large, well-circumscribed heterogeneous mass lesion is observed with nonspecific appearance.
- Characteristic "bowl of fruit" sign on T2-weighted MRI due to the presence of multiple tissue components is observed.

Lymphoid Tumors

Lymphoma

Lymphoma accounts for 33% of all primary retroperitoneal tumors.[1,7] It can be broadly classified as Hodgkin disease (HD) and non-Hodgkin lymphoma (NHL). HD usually involves the mediastinum and spleen with a bimodal age distribution with peaks in the second and sixth decades. NHL is seen in older patients in the 40 to 70 year age group and often involves extra-nodal sites like the liver, spleen, and intestines.[7] Paraaortic lymph nodes are involved in 25% of patients with HD and 55% of patients with NHL. Approximately 14% of patients with NHL present with a dominant retroperitoneal mass.[9]

On CT, lymphoma is seen as a well-defined, homogenous soft-tissue attenuation para-aortic or pelvic mass with minimal contrast enhancement. Necrosis and calcification are uncommon before therapy.[5,7] It is infiltrative and often appears as a mantle-like mass and tends to spread between normal retroperitoneal structures, surrounding and engulfing vessels (aorta and IVC) without compressing their lumen giving the "CT angiogram" sign (►**Fig. 10**). The "floating aorta" sign may be noted due to the encasement and displacement of the aorta anteriorly by the tumor.[21] This sign is the characteristic of lymphoma and is generally not seen in other retroperitoneal tumors.[5] On MRI, the mass is typically isointense to muscle on T1-weighted images. On T2-weighted images, it is seen to be iso- to hyperintense and shows moderate homogeneous contrast enhancement. Homogeneous appearance on both enhanced and unenhanced scans is the main distinguishing factor for lymphoma. However,

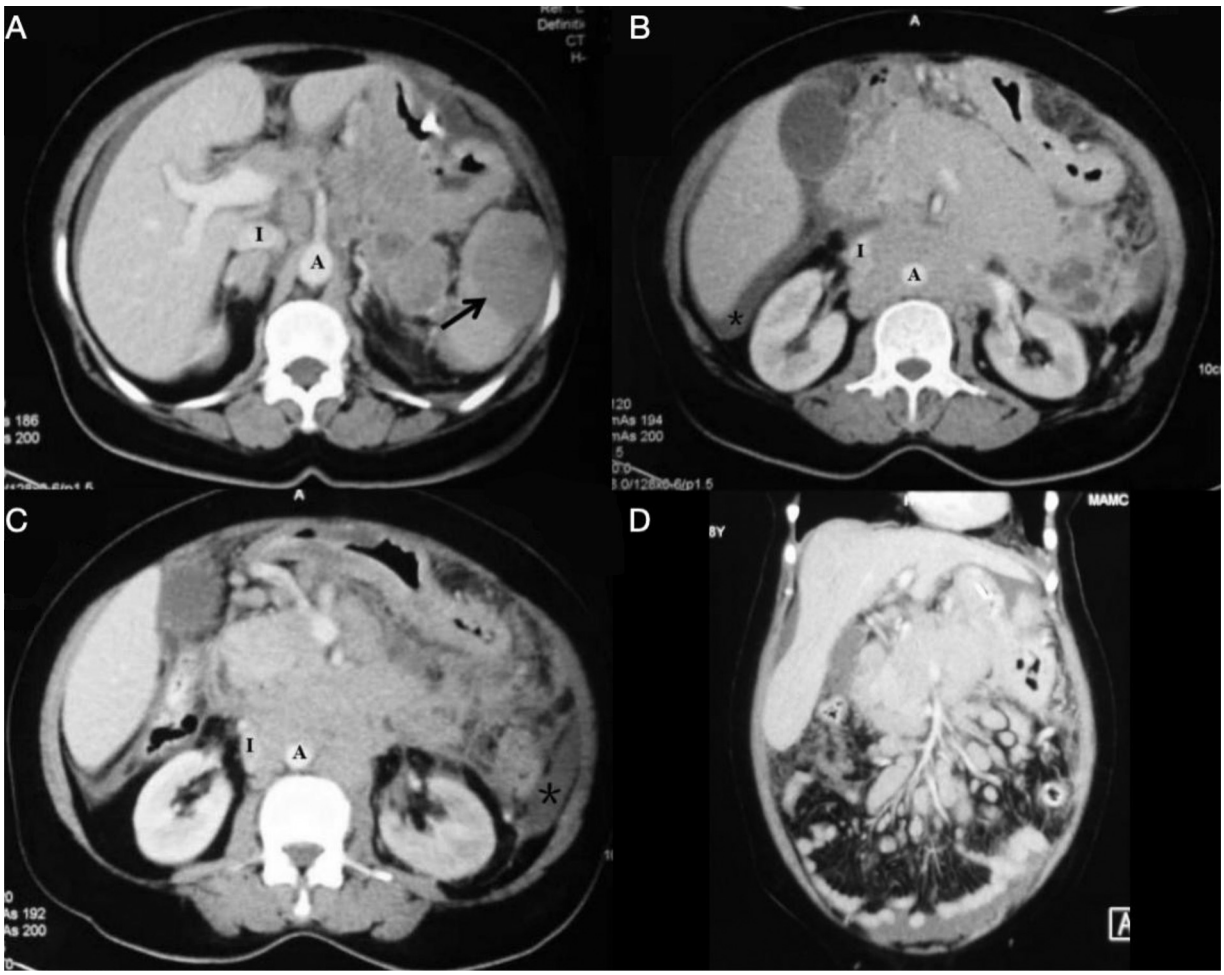

Fig. 10 Retroperitoneal lymphadenopathy in a 48-year-old woman with Non-Hodgkin's lymphoma. (**A**, **B**, **C**) Axial post-contrast CT images demonstrate a homogeneously enhancing lymph node conglomerate in the retroperitoneum that anteriorly displaces the IVC (I) and surrounds abdominal aorta (A). The pancreas is also involved and is not visualized separately from the lesion. Note the lymphomatous deposit in the spleen (*small arrow*) and mild ascites (*asterisk*). (**D**) Coronal CT image shows encasement of the superior mesenteric artery by the lymph nodal mass with extensive mesenteric lymphadenopathy.

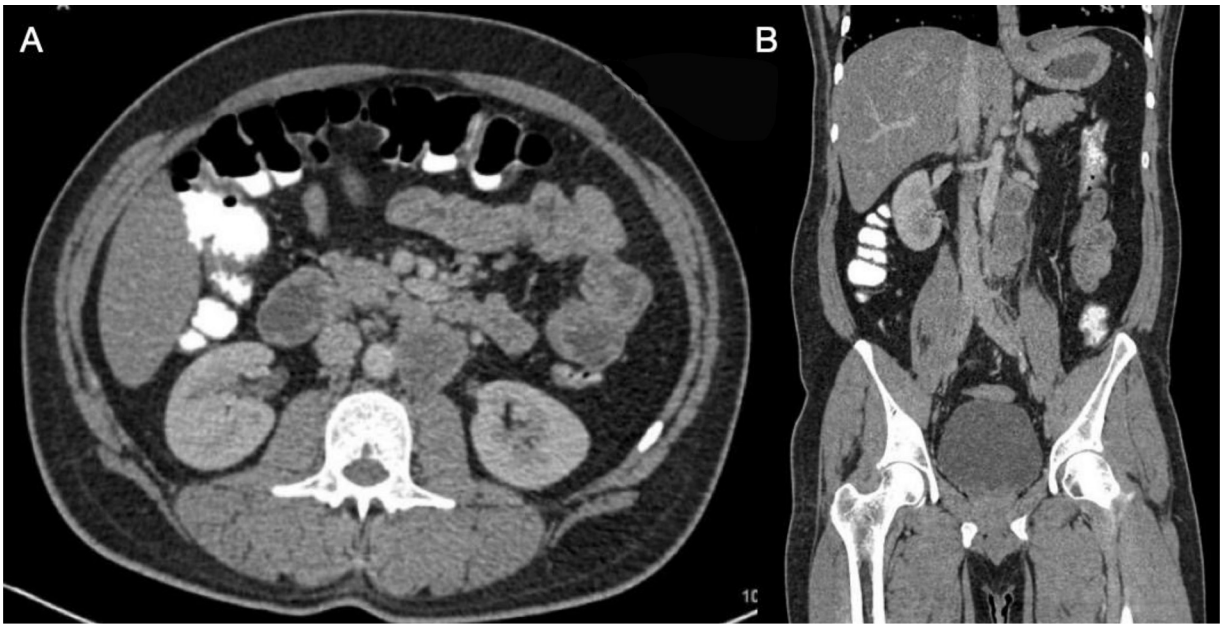

Fig. 11 Retroperitoneal lymphadenopathy in a 37-year-old male with metastatic testicular carcinoma. (**A**) Axial and (**B**) coronal post-contrast CT images through the abdomen reveal multiple enlarged retroperitoneal lymph nodes in the paracaval and left paraaortic locations with heterogeneous peripheral enhancement and central necrosis.

about 23% of NHL are heterogeneous and cannot be distinguished from other primary nonlipomatous retroperitoneal tumors.[7]

Lymphoma is treated with chemotherapy, radiation therapy, and/or immunotherapy.[22] Soft-tissue masses continue to persist after therapy because of fibrosis or viable tumor. MRI and positron emission tomography (PET) scans may be used to differentiate between fibrosis and residual tumor; fibrosis is seen as low signal intensity on T2-weighted imaging, has minimal enhancement, and does not take up fluorodeoxyglucose on PET scans.[1]

Post-transplantation lymphoproliferative disease (PTLD) is a rare disorder seen in solid organ transplant recipients that can affect lymph nodes or extranodal organs. Retroperitoneum is one of the common locations of the nodal form. It may present as either retroperitoneal lymphadenopathy or an ill-defined infiltrative mass.[23]

Extramedullary plasmacytoma (EMP) is a rare type of plasma cell neoplasm arising primarily in soft tissues with normal bone marrow. It can be rarely seen in the retroperitoneum in perinephric location. Imaging morphology is nonspecific and presents as either a well-circumscribed focal mass or an extensive, infiltrating soft-tissue mass with homogeneous contrast enhancement.[1]

Metastatic lymphadenopathy to retroperitoneum is also a common occurrence and may be difficult to differentiate from lymphoma based on imaging findings alone. Renal cell, cervical, testicular, and prostatic carcinomas are common primary malignancies that present with metastatic retroperitoneal lymphadenopathy.[5,7] The imaging appearance is variable, from discrete enlarged nodes to a single conglomerate mass. A history of primary malignancy and the presence of necrosis suggest metastatic lymphadenopathy (►**Fig. 11**).

Lymphoma
- Well-defined, homogeneous para-aortic or pelvic masses are observed with minimal contrast enhancement.
- Infiltrative mantle-like growth is observed with the encasement of aorta and IVC without luminal compression.
- "CT angiogram" sign or "floating aorta" sign are characteristics.

Neurogenic Tumors

In the retroperitoneal region, neurogenic tumors represent 10 to 20% of all primary retroperitoneal tumors and may originate from the nerve sheath, ganglionic cells, or paraganglionic system.[1,7,24] Schwannoma and neurofibroma are tumors of nerve sheath origin. Ganglioneuroma, ganglioneuroblastoma, and neuroblastoma are the tumors arising from ganglion cells, whereas paraganglioma and extra-adrenal pheochromocytoma arise from the paraganglionic system.

Schwannoma

Schwannoma or neurilemmoma is an encapsulated, circumscribed tumor arising from well-differentiated Schwann cells. It is twice as common in females as compared to males and tends to affect people between the ages of 20 to 50 years.[25] Usually occurring in the head and neck regions, and in the upper extremities, it rarely occurs in the retroperitoneum. Retroperitoneal schwannomas account for up to 6% of all retroperitoneal tumors.[1] Typically, it is solitary and benign; however, multiple masses may be present, particularly in association with neurofibromatosis type-2 (NF-2). It is insensitive to radiation and chemotherapy, and surgical excision remains the primary treatment of choice.

The mass tends to run along peripheral nerves in the presacral and paravertebral retroperitoneal space and has smooth, well-defined borders, and oval or spherical shape.[25] It usually demonstrates homogeneous attenuation on non-contrast CT; however, heterogeneous enhancement may be seen due to cystic degeneration particularly when the tumor is large (►**Fig. 12**). It may show areas of punctate or curvilinear calcifications. On MR, a schwannoma shows low-to-intermediate intensity on T1- and iso- to high signal intensity on T2-weighted imaging with solid enhancing components and a hypointense capsule (►**Fig. 12**).[7,25] Target-like appearance on T2-weighted images and target-like post-contrast enhancement described for neurofibromas may occasionally be seen in schwannomas as well. Ancient schwannoma refers to a large, long-standing tumor with advanced degenerative changes (cystic degeneration, calcification, and hemorrhagic areas).[25]

Schwannoma
- Well-circumscribed homogenous mass is observed along peripheral nerves in the presacral and paravertebral regions.
- Cystic degeneration may be seen in old, large tumors leading to heterogeneous enhancement.

Neurofibroma

Neurofibroma is a benign unencapsulated neural sheath tumor, accounting for only 1% of retroperitoneal tumors.[7] It is usually seen in the second to fourth decades of life and occurs more commonly in men. It is usually a solitary tumor. Multiple neurofibromas are usually seen in association with NF-1.[2,25] Malignant degeneration is more common in neurofibromas compared to schwannomas, especially when associated with neurofibromatosis. Symptoms of abdominal neurofibroma include a palpable abdominal mass or pain along the distribution of a nerve; however, about 65% of cases are asymptomatic.[26]

Retroperitoneal neurofibroma is seen as a well-defined, round, or fusiform, hypodense (20–25 HU), homogeneous solid mass along the course of a nerve on CT.[1] Typically, there is homogeneous contrast enhancement (30–50 HU) in the lesion; sometimes cystic non-enhancing areas due to myxoid degeneration may be seen. When it originates from the spinal nerve root, a dumbbell-shaped lesion with associated enlargement of the neural foramen is usually present (►**Fig. 13**). Neurofibroma has low signal intensity on T1- and iso- to high- signal intensity on T2-weighted MRI. On T2-weighted images, a characteristic "target" appearance may be seen with central low signal intensity and peripheral high signal intensity corresponding to the central core of fibrous

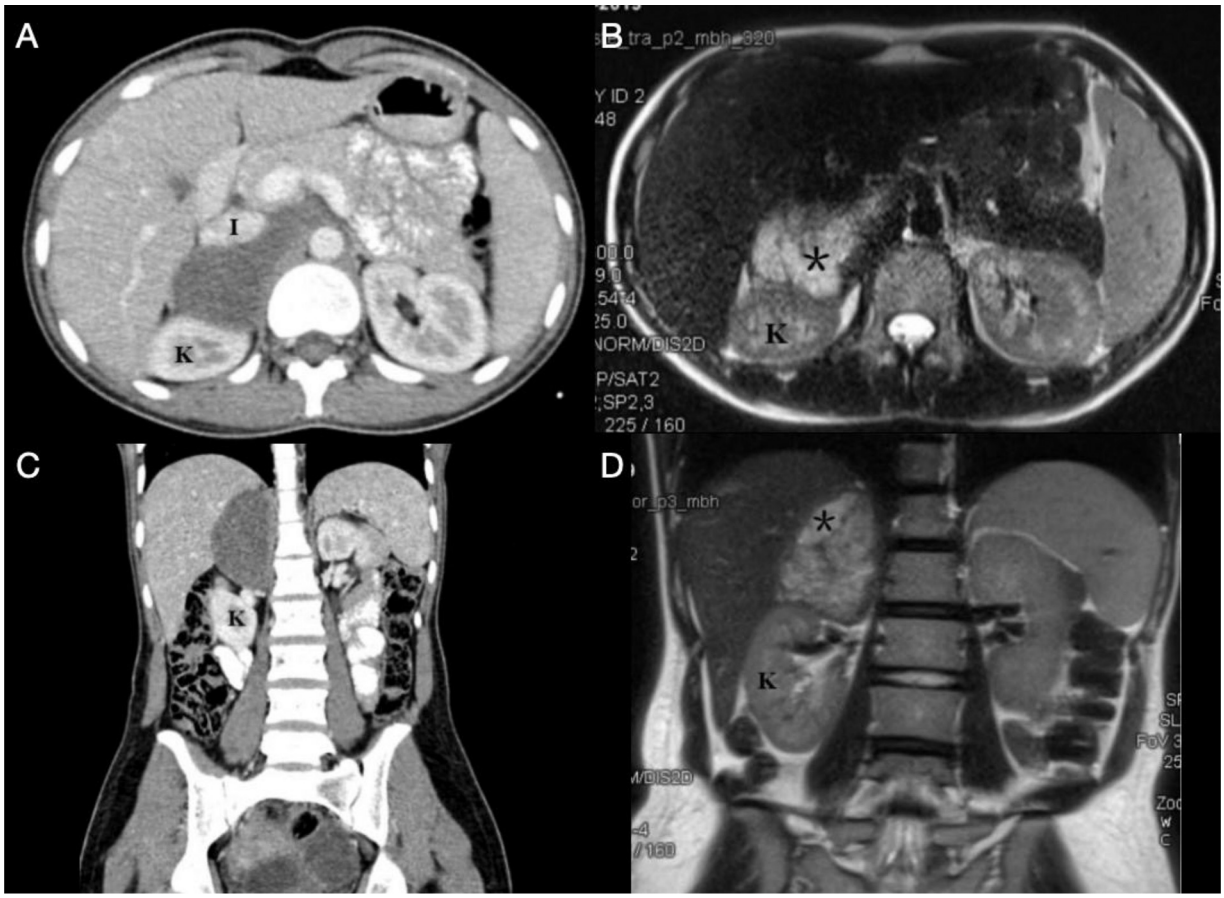

Fig. 12 Post-contrast CT and T2-weighted MRI (**A**, **B**) axial and (**C**, **D**) coronal images of a 17-year-old girl demonstrate a circumscribed homogenous retroperitoneal mass in the right paravertebral region. The mass displaces the right kidney (K) postero-inferiorly and IVC (I) anteriorly. High signal intensity areas (*asterisk*) correspond to areas of cystic/myxoid degeneration. Characteristic location, CT, and MRI appearance suggest a retroperitoneal neurogenic tumor, likely Schwannoma.

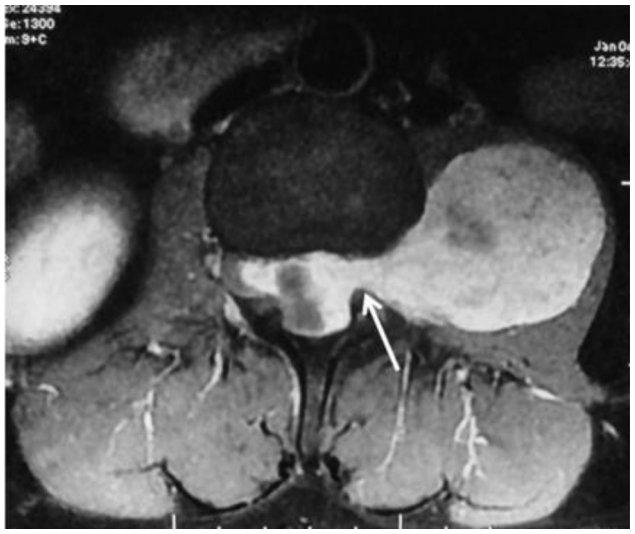

Fig. 13 Retroperitoneal neurofibroma in a 39-year-old female. Contrast-enhanced axial T1- weighted MRI demonstrates a well-defined homogeneously enhancing mass lesion in the left paravertebral region, which displaces the left psoas muscle postero-laterally. There is a dumbbell-shaped intraspinal extension of the lesion with widening of the neural foramen (*white arrow*).

tissue and peripheral myxoid component.[27] The target pattern of central enhancement may also be seen in post-contrast images.

Plexiform neurofibroma in the retroperitoneum is seen as a large, extensive infiltrating mass in a para-psoas or presacral location, symmetrically extending along the lumbosacral plexus. It is almost exclusively seen with NF-1 and seen as a hypodense mass on CT owing to the presence of myxoid tissue, adipose tissue, and Schwann cells.[2]

Neurofibroma
- Well-defined round or fusiform solid mass is observed along the course of a nerve with homogenous contrast enhancement. Dumbbell shape and foraminal widening are seen when neural foraminal extension is present.
- Characteristic "target" appearance on T2-weighted MRI may be seen.

Malignant Peripheral Nerve Sheath Tumor

It is a highly aggressive and infiltrative tumor, with a high incidence of distant metastases and recurrence. Approximately, 50% of cases of malignant peripheral nerve sheath tumor (MPNST) are seen in association with NF-1. The most common location of an MPNST in the retroperitoneum is the paraspinal region.[2] Imaging is not reliable in differentiating between a benign and malignant nerve sheath tumor. However, gross tumor inhomogeneity with necrotic areas, irregular/infiltrative borders with the invasion of surrounding structures, and destruction of adjacent bones are some features helpful in differentiation (►**Fig. 14**).[2,25]

Malignant peripheral nerve sheath tumor
- Nonspecific imaging appearance.
- Heterogeneous necrotic mass with irregular borders and invasion of surrounding structures usually located in the paraspinal region are observed.

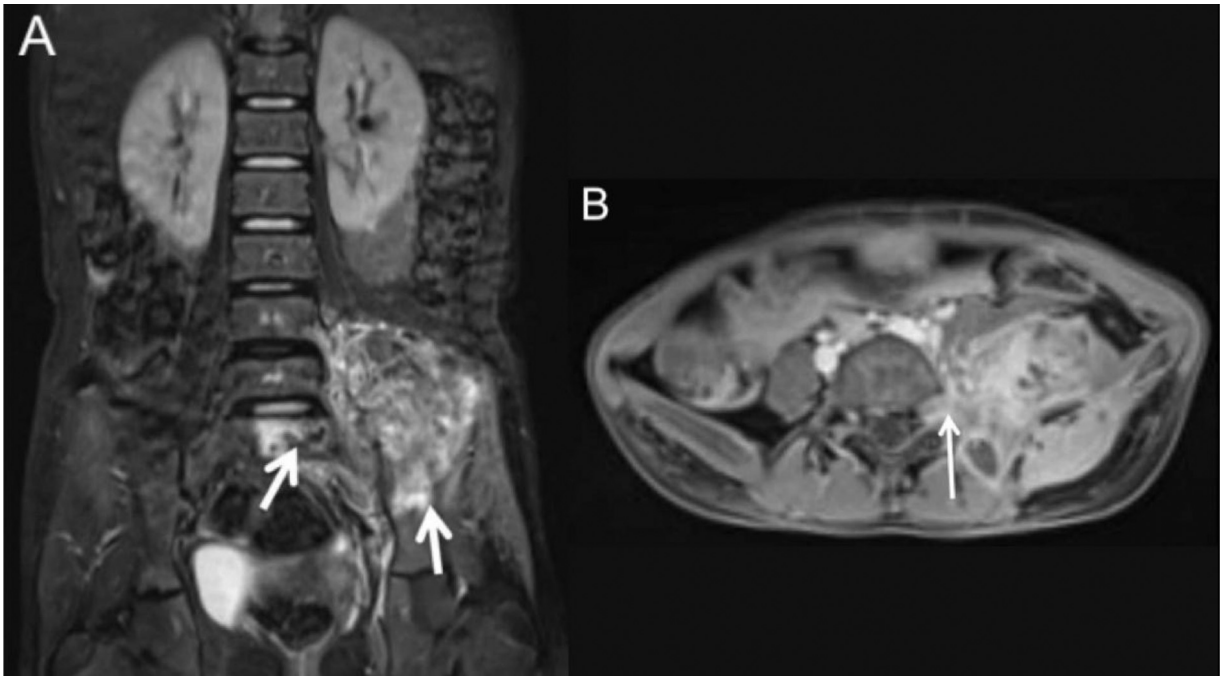

Fig. 14 Malignant peripheral nerve sheath tumor in a 28-year-old female. Fat saturated T2-weighted (**A**) coronal and (**B**) post-contrast T1-weighted axial MRI show an ill-defined infiltrative heterogeneous mass lesion involving the left lumbosacral plexus with intraspinal component (*long white arrow*). The lesion appears heterogeneously hyperintense on T2-weighted images with heterogeneous post-contrast enhancement and areas of necrosis. The lesion is invading the left iliac bone and sacrum (*short white arrows*).

Ganglioneuroma

Ganglioneuroma is a rare benign, slow-growing tumor usually seen in the 20 to 40-year age group afflicting both sexes equally.[28,29] Patients are either asymptomatic or present with abdominal pain and a palpable mass. Sometimes symptoms such as hypertension, diarrhea, and virilization may be seen due to the secretion of catecholamines and androgens.[30] It can arise anywhere along the paravertebral sympathetic plexus but is most commonly localized to the retroperitoneum and mediastinum.

On CT, a ganglioneuroma is seen as a well-circumscribed, longitudinally oriented paravertebral hypoattenuating mass that often surrounds blood vessels without compressing them. The lesion may have calcifications (20–30% cases) that are discrete and well-defined, unlike the amorphous and coarse calcifications of neuroblastomas.[31] It also has more calcifications compared to nerve sheath tumors.[1] However, hemorrhage and necrosis are very uncommon. Varying degrees of contrast enhancement have been reported. A delayed heterogeneous contrast enhancement pattern has also been described, explained by the myxoid matrix of the tumor which results in delayed, slow accumulation of contrast material in the extracellular space.[31] The lesion is homogenous and has low signal intensity on T1-weighted MRI. Appearance on T2-weighted images depends on the proportion of the myxoid, cellular, and collagen components. Masses with large amounts of myxoid stroma show markedly increased T2 signal intensity. It may give a characteristic "whorled" appearance on T2-weighted imaging as curvilinear bands of low signal intensity in the lesion due to the longitudinal and transverse arrangement of Schwann cells and collagen fibers within the tumor.[32]

Surgical resection is the treatment of choice for ganglioneuroma, and recurrence is rare.[33]

Ganglioneuroma
- Longitudinally oriented paravertebral mass surrounding vessels without compression, often with calcifications, is seen in adolescents and young adults.
- T2-weighted MRIs show a whorled appearance.

Paraganglioma

A paraganglioma is a rare, highly vascular, and often heritable neuroendocrine neoplasm originating from neuroendocrine cells scattered throughout the body. In the retroperitoneum, it arises from extra-adrenal neural crest cells distributed along the aorta. The most common location is near the origin of the inferior mesenteric artery, at the organ of Zuckerkandl, the most prominent collection of paraganglionic tissue in the region.[34] It is more aggressive than an adrenal pheochromocytoma and is malignant in up to 40% of cases.[5] Some patients may even present with distant metastases, with lung, liver, and bones being the common sites.[35,36] It is primarily seen in the third to fourth decades of life and has an equal incidence in males and females. Retroperitoneal paraganglioma is functional in about 60% of cases; these are detected earlier owing to the symptoms of catecholamine excess such as episodic hypertension, tachycardia, and diaphoresis.[5] On CT, the lesion is seen as a well-circumscribed paraaortic soft-tissue mass with homogenous intense central enhancement. There may be central areas of necrosis. Focal areas of high attenuation due to hemorrhage and areas of punctate calcification may also be seen. CT imaging features of paragangliomas may overlap with those of other retroperitoneal masses, especially those of neural and mesodermal origin. The close relationship of the tumors to the aorta is of some value in differentiating them from other retroperitoneal tumors. Correlation of symptoms and urinary catecholamine levels in a patient with a soft-tissue mass in the retroperitoneum on CT aids in arriving at the correct diagnosis. Diagnosing a non-functional paraganglioma is challenging. MRI is preferred over CT in suspected paragangliomas owing to better tissue differentiation and lack of radiation. The lesions are hypo- or isointense to liver parenchyma on T1-weighted imaging and markedly hyperintense on T2-weighted imaging with brisk enhancement on post-contrast images (►**Fig. 15**). About 80% of cases show the characteristic uniform high signal intensity on T2-weighted images (light bulb sign); the presence of internal hemorrhage may reduce T2 signal intensity in the remaining cases.[2] The tumors are highly vascular and show an intense tumor blush with enlarged feeding arteries on angiography. On MRI, features like necrosis and avid contrast enhancement during the arterial phase are highly suggestive of extra-adrenal paragangliomas and help to differentiate them from schwannoma.[35] There are no imaging characteristics that can reliably differentiate benign and malignant paragangliomas; however, the presence of local invasion and distant metastases suggests malignancy.[7] Functional imaging with metaiodobenzylguanidine scintigraphy helps differentiate functional from non-functional tumors and in the detection of multiple primary tumors and metastases.[36]

Paraganglioma
- Well-circumscribed mass is seen close to the aorta with mostly homogenous intense post-contrast enhancement.
- Characteristic uniform high signal intensity on T2-weighted images (light bulb sign) may be seen.

Germ Cell Tumors

Primary Extragonadal Germ Cell and Sex Cord-Stromal Tumors

These are an uncommon group of germ cell tumors arising from aberrant primordial germ cell rests or ectopic sex cord-stromal tissue in the retroperitoneum. Primary gonadal tumors should be ruled out first as retroperitoneal metastases are seen in about 30% of primary gonadal tumors and form the majority of retroperitoneal germ cell tumors.[1] Extragonadal germ cell tumors can be seminomas or non-seminomatous tumors, which include embryonal carcinoma, yolk sac tumor, choriocarcinoma, and mixed germ cell tumors. These are often seen in or near the midline, usually between sixth thoracic and second sacral vertebrae.[1] Imaging morphology is nonspecific in both groups of tumors, and

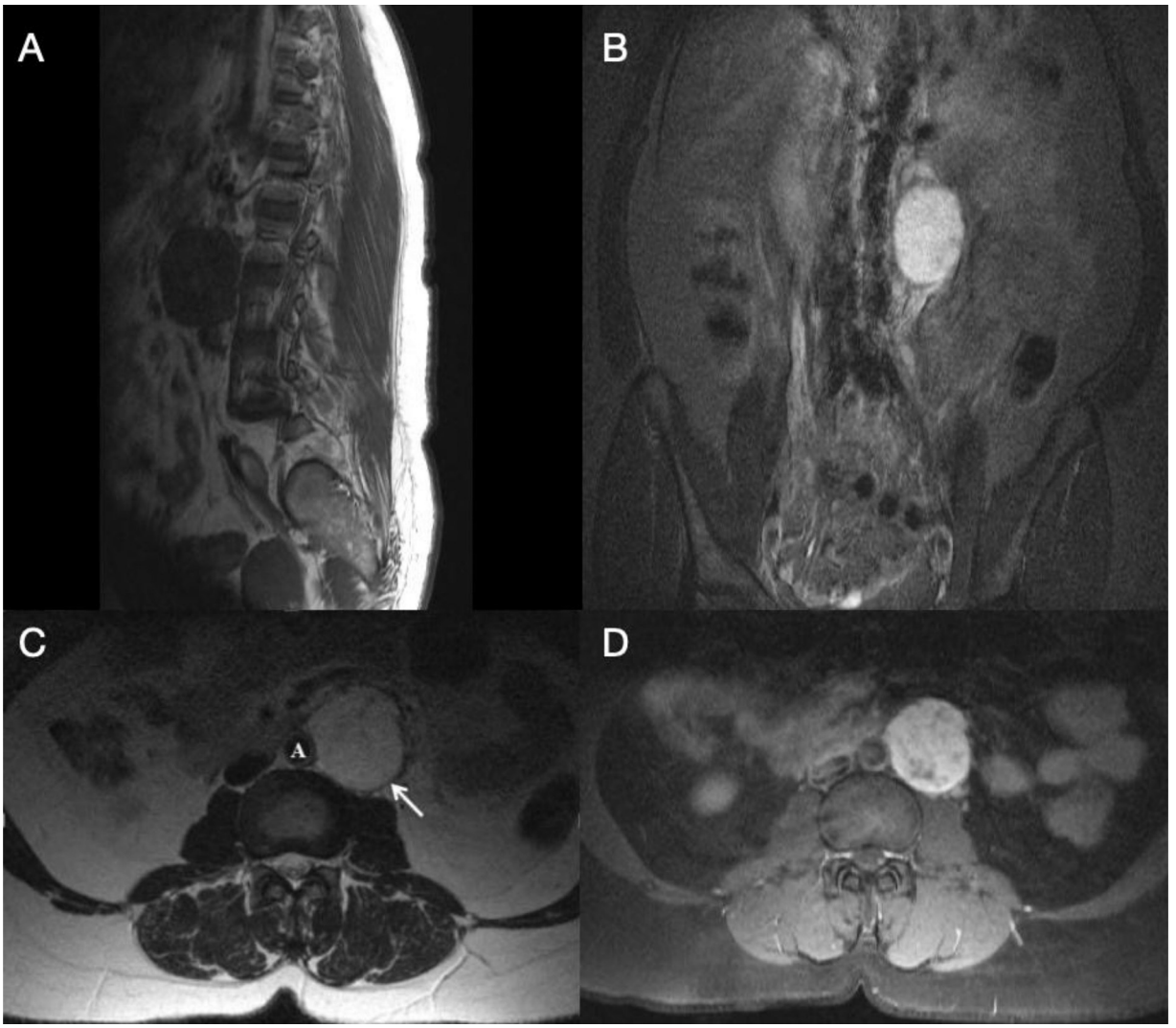

Fig. 15 Retroperitoneal paraganglioma in a 41-year-old female with hypertension. (**A**) T1-weighted sagittal, (**B**) fat-saturated T2-weighted coronal, and (**C**) T2-weighted axial MRI show a circumscribed, retroperitoneal mass lesion in the left para-aortic prevertebral location with homogenous low to intermediate T1 signal intensity and high T2 signal intensity. A low signal intensity peripheral capsule can also be appreciated on T2-weighted images. (**D**) Fat suppressed, contrast-enhanced T1-weighted axial MRI demonstrates moderate to high, relatively homogenous enhancement in the lesion.

they appear as well-defined homogenous or heterogeneous soft-tissue masses with variable enhancement patterns.

Primary extragonadal germ cell and sex cord-stromal tumors
- Nonspecific morphology on imaging but most appear as well-defined homogenous or heterogeneous soft-tissue masses with variable enhancement patterns seen in/near the midline between the lower thoracic to sacral vertebrae.
- Primary gonadal germ tumors need to be ruled out first as retroperitoneal metastasis from these tumors is much more common than primary extragonadal germ cell tumors.

Non-Neoplastic Lesions

Extramedullary Hematopoiesis

EMH is a compensatory mechanism for hematopoiesis, when there is reduced bone marrow in conditions such as hemoglobinopathies, leukemias, myelofibrosis, lymphomas, and carcinomas. EMH is commonly seen in the liver, spleen, and lymph nodes but can be seen in any organ of mesenchymal origin. It may be rarely seen in the retroperitoneum around the kidneys, within paravertebral tissues, and sometimes in the kidneys.[1,5]

On CT, lesions are seen as multiple symmetrical, round, or lobulated, iso- or hyperattenuating soft-tissue masses in the paravertebral region with minimal post-contrast enhancement (►**Fig. 16**). Macroscopic fat may be seen in some cases. There is usually no associated bone destruction or calcification. Bones show widened diploic space as a secondary sign of anemia. The appearance on MRI is variable. The red marrow and hemosiderin content result in low signal intensity on T1- and T2- weighted images, whereas high intensity may be seen on T1- and T2- images due to the presence of fatty tissue. The typical imaging appearance of perirenal EMH is the soft tissue surrounding the kidneys without affecting the renal contour.[37] Characteristics accompanying

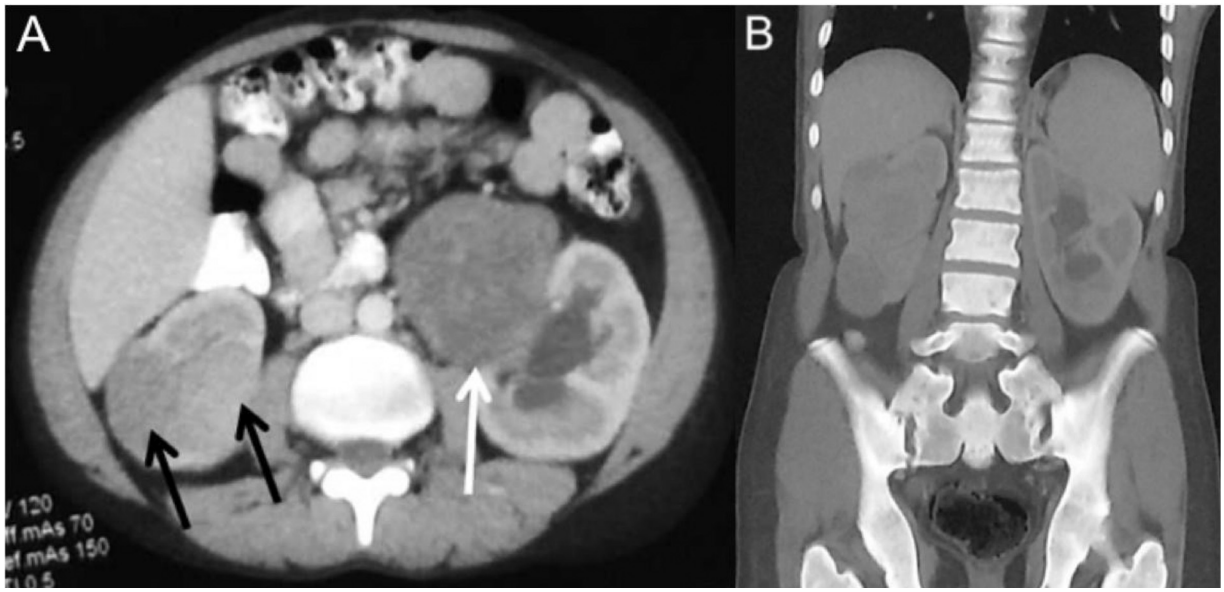

Fig. 16 Retroperitoneal extramedullary hematopoiesis in a 20-year-old female with myelofibrosis. (**A**) Contrast-enhanced axial CT image shows a well-defined, round, minimally enhancing soft-tissue mass lesion (*white arrow*) in the left perinephric space of the retroperitoneum. The lesion is compressing the left pelvi-ureteric junction with mild hydronephrosis. Similar appearing multiple lobulated mass lesions also noted involving the right kidney (*black arrows*). (**B**) Coronal bone window CT image demonstrates diffusely increased density of the axial skeleton (osteosclerosis) due to myelofibrosis.

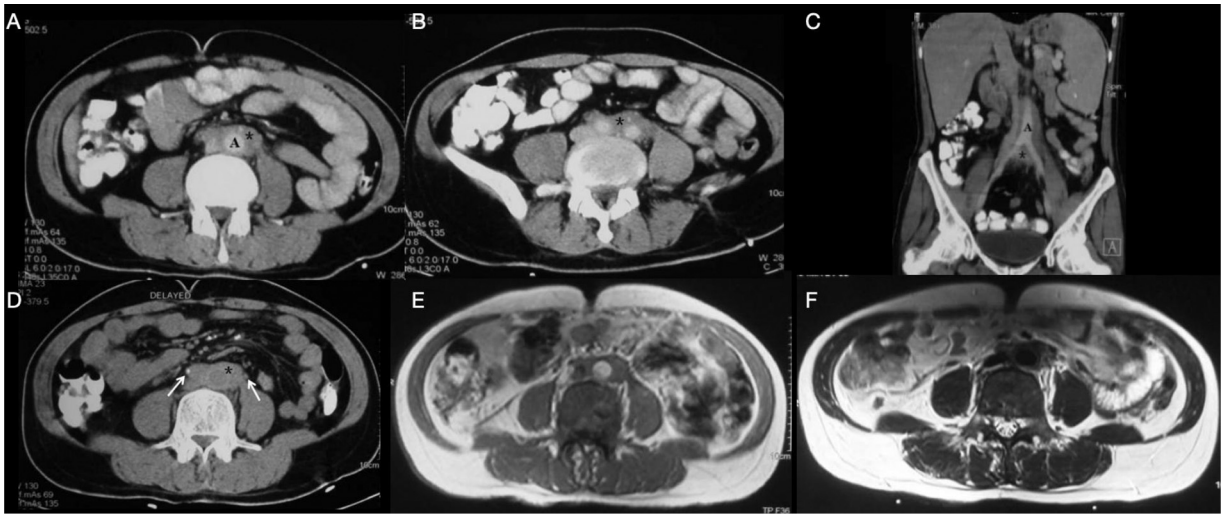

Fig. 17 Idiopathic retroperitoneal fibrosis in a 38-year-old man. (**A**, **B**) Contrast-enhanced axial and (**C**) coronal CT images demonstrate a well-defined, retroperitoneal, soft-tissue mass (*asterisk*) surrounding the infrarenal abdominal aorta (A) and extending inferiorly to involve the common iliac arteries bilaterally. (**D**) Delayed excretory phase axial CT image shows partial encasement with narrowing of both ureters (*arrows*) with hydronephrosis (*not shown*). (**E**) Axial T1- and (**F**) T2-weighted MRI show intermediate T1 signal and low T2 signal intensity, indicative of mature fibrosis.

bone changes in a patient with known hemoglobinopathy are diagnostic. However, a biopsy is often necessary to exclude lymphoma or ECD, both of which can also have a similar appearance.[37]

Extramedullary Hematopoiesis
- Multiple rounds or lobulated paravertebral or perinephric soft-tissue masses are observed, with minimal post-contrast enhancement.
- Characteristics of bone change with widened diploic spaces.

Retroperitoneal Fibrosis

RPF is a rare collagen disorder that can mimic a retroperitoneal tumor. It is seen as a mass usually centered around the aorta, IVC, and iliac vessels due to the proliferation of fibrous plaques. Two-third of the cases are idiopathic and the rest are secondary to certain medications, neoplasms, radiation, chemotherapy, aortic aneurysms, and infections like tuberculosis.[38] RPF is more common in males and is usually seen in the age group of 40 to 60 years.[7] In the early stages, RPF can be asymptomatic, but patients may present with symptoms such as pain, swelling of extremities,

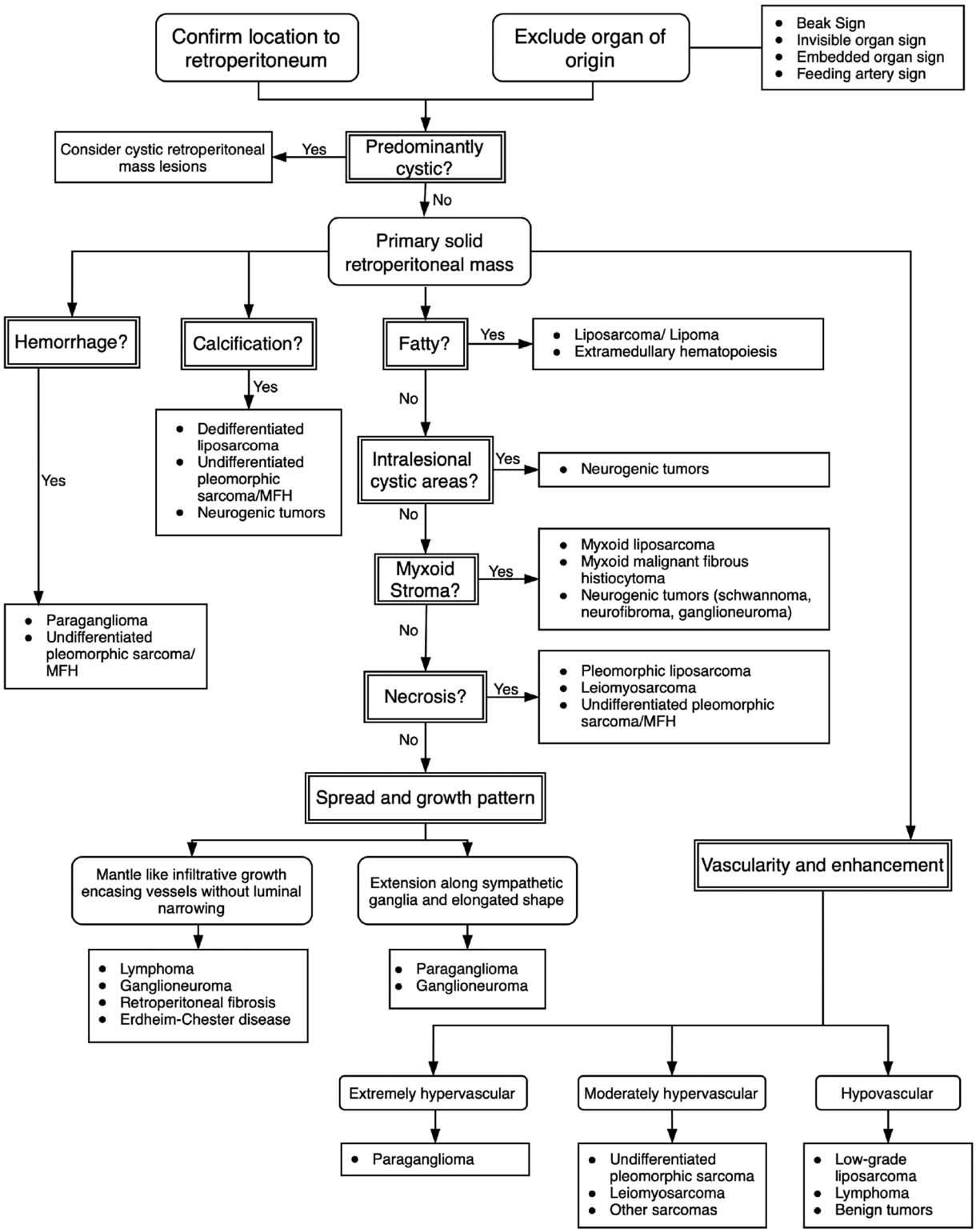

Fig. 18 Diagnostic algorithm for primary retroperitoneal solid lesions.

testicular swelling, and reduction in urine output as the disease progresses.[1]

On CT, plaque-like, irregular, and ill-defined soft-tissue masses are seen in the retroperitoneum, most commonly surrounding the infrarenal abdominal aorta and proximal common iliac arteries and involving other structures including the ureters, duodenum, pancreas, and spleen (►**Fig. 17**). Unlike lymphomatous masses, these lesions do not displace the structures anteriorly but encase them. In the initial inflammatory active stage, early and avid enhancement is seen, but as the disease progresses to fibrosis, delayed enhancement is noted. The appearance on T2-weighted images and enhancement depends on the amount of edema and inflammation. MRI shows high signal

intensity on T2-weighted images in the acute phase of the disease, with early contrast enhancement, and shows low signal intensity in the chronic fibrosing phase with delayed enhancement (►**Fig. 17**).[1,38] Corticosteroid therapy is the mainstay of treatment. The decrease in T2 signal intensity and enhancement is also brought about with effective therapy and is valuable in assessing response to treatment.[38]

Retroperitoneal Fibrosis
- Ill-defined soft-tissue masses near infra-renal abdominal aorta encase surrounding structures without invading them.
- Early inflammatory stages show T2 hyperintense signal and strong post-contrast enhancement, and later stages show low T2 signal and delayed enhancement with increasing fibrosis.

Erdheim-Chester Disease

ECD is a rare multisystem disorder that usually affects adults in the fifth to seventh decades of life. It is a form of non-Langerhans cell histiocytosis, and most commonly involves the skeletal system leading to osteosclerosis and bone pain. About 50% of patients with ECD have extra-skeletal disease and the infiltrates may involve the brain, lungs, orbits, and retroperitoneum.[39] Clinical manifestations depend upon the sites involved and often include diabetes insipidus, proptosis, histiocytic skin lesions or ureteric obstruction, and renal failure.[40] On imaging, retroperitoneal involvement is seen as symmetric, bilateral, peri- and pararenal rind of soft tissue, and proximal ureteric infiltration, often leading to ureteric obstruction and subsequent renal failure.[7] The soft tissue appears homogeneous and hypoattenuating on CT and shows weak contrast enhancement. Low signal intensity is seen on both T1- and T2-weighted MRI with minimal contrast enhancement.[1,7] Diagnosis is aided by the characteristic radiographic findings of symmetric osteosclerosis in the dia-metaphyseal regions of long bones with relative sparing of the axial skeleton and epiphyseal regions.[40] ECD can be differentiated from primary RPF by the presence of hairy kidneys (symmetrical and bilateral dense infiltration of the perinephric space), coated aorta (circumferential periaortic involvement), and also by the absence of involvement of pelvic ureter and IVC.[5]

ECD
- Bilateral homogeneous perirenal hypoattenuating masses are observed on CT with weak contrast enhancement, often with ureteric infiltration.
- Low signal intensity on both T1- and T2W- images with minimal contrast enhancement is observed.

Algorithmic Approach

An algorithmic approach to a primary retroperitoneal solid mass is presented here that can help characterize a lesion and narrow down the differential diagnosis (►**Fig. 18**). After confirming the location and excluding any organ of origin, the lesion should first be classified as predominantly solid or cystic. Once a predominantly solid primary retroperitoneal mass is confirmed, further classification on the basis of the presence of calcifications, hemorrhagic areas, fatty areas, and vascularity can be done to narrow the differentials. If the lesion does not seem to fit in any of these broad categories- characteristics such as the presence of myxoid stroma, necrosis, intralesional cystic areas, and the spread and growth pattern of the mass are useful factors in reaching a diagnosis.

Conclusion

Primary solid retroperitoneal lesions are rare and constitute a diverse group of lesions. They pose a diagnostic challenge due to overlapping and nonspecific imaging findings. Knowledge about retroperitoneal anatomy, key radiological and clinical features, and a systematic approach to such lesions helps the radiologist narrow the differential diagnosis and delineate the entire extent aiding management.

Disclosures
None.

Conflicts of Interest
None declared.

References

1 Rajiah P, Sinha R, Cuevas C, Dubinsky TJ, Bush WH Jr, Kolokythas O. Imaging of uncommon retroperitoneal masses. Radiographics 2011;31(04):949–976
2 Brennan C, Kajal D, Khalili K, Ghai S. Solid malignant retroperitoneal masses—a pictorial review. Insights Imaging 2014;5(01):53–65
3 Osman S, Lehnert BE, Elojeimy S, et al. A comprehensive review of the retroperitoneal anatomy, neoplasms, and pattern of disease spread. Curr Probl Diagn Radiol 2013;42(05):191–208
4 Ishikawa K, Nakao S, Nakamuro M, Huang TP, Nakano H. The retroperitoneal interfascial planes: current overview and future perspectives. Acute Med Surg 2016;3(03):219–229
5 Goenka AH, Shah SN, Remer EM. Imaging of the retroperitoneum. Radiol Clin North Am 2012;50(02):333–355, vii
6 Filippone A, Cianci R, Cotroneo AR. Mesenteric and retroperitoneal diseases. In: Zech CJ, Bartolozzi C, Baron R, Reiser MF, eds. Multislice-CT of the Abdomen. Berlin, Heidelberg: Springer; 2012:321–36
7 Scali EP, Chandler TM, Heffernan EJ, Coyle J, Harris AC, Chang SD. Primary retroperitoneal masses: what is the differential diagnosis? Abdom Imaging 2015;40(06):1887–1903
8 Shaaban AM, Rezvani M, Tubay M, Elsayes KM, Woodward PJ, Menias CO. Fat-containing retroperitoneal lesions: imaging characteristics, localization, and differential diagnosis. Radiographics 2016;36(03):710–734
9 Neville A, Herts BR. CT characteristics of primary retroperitoneal neoplasms. Crit Rev Computed Tomogr 2004;45(04):247–270
10 Sassa N. Retroperitoneal tumors: review of diagnosis and management. Int J Urol 2020;27(12):1058–1070
11 Messiou C, Moskovic E, Vanel D, et al. Primary retroperitoneal soft tissue sarcoma: imaging appearances, pitfalls and diagnostic algorithm. Eur J Surg Oncol 2017;43(07):1191–1198
12 Craig WD, Fanburg-Smith JC, Henry LR, Guerrero R, Barton JH. Fat-containing lesions of the retroperitoneum: radiologic-pathologic correlation. Radiographics 2009;29(01):261–290

13 Rekhi B, Navale P, Jambhekar NA. Critical histopathological analysis of 25 dedifferentiated liposarcomas, including uncommon variants, reviewed at a Tertiary Cancer Referral Center. Indian J Pathol Microbiol 2012;55(03):294–302
14 O'Regan KN, Jagannathan J, Krajewski K, et al. Imaging of liposarcoma: classification, patterns of tumor recurrence, and response to treatment. AJR Am J Roentgenol 2011;197(01):W37-43
15 Al-Ani Z, Fernando M, Wilkinson V, Kotnis N. The management of deep-seated, lowgrade lipomatous lesions. Br J Radiol 2018;91 (1086):20170725
16 Shin NY, Kim M-J, Chung J-J, Chung Y-E, Choi J-Y, Park Y-N. The differential imaging features of fat-containing tumors in the peritoneal cavity and retroperitoneum: the radiologic-pathologic correlation. Korean J Radiol 2010;11(03):333–345
17 Park JO, Qin L-X, Prete FP, Antonescu C, Brennan MF, Singer S. Predicting outcome by growth rate of locally recurrent retroperitoneal liposarcoma: the one centimeter per month rule. Ann Surg 2009;250(06):977–982
18 Aftan MK, Alfalahi A, Alzeena E, Albastaki U, Houcinat Y, Mahmoud K. Leiomyosarcoma: a rare presentation as multifocal lesion. BJR Case Rep 2020;6(03):20190117
19 Choi JH, Ro JY. Retroperitoneal sarcomas: an update on the diagnostic pathology approach. Diagnostics (Basel) 2020;10(09):E642
20 Narula MK, Madan R, Pathania OP, Anand R. Primary intra-abdominal synovial sarcoma. Appl Radiol 2007;36:48A–48D Accessed March 9, 2021 at: https://appliedradiology.com/articles/primary-intra-abdominal-synovial-sarcoma
21 Acar T, Harman M, Guneyli S, et al. Cross-sectional imaging features of primary retroperitoneal tumors and their subsequent treatment. J Clin Imaging Sci 2015;5:24
22 Jamil A, Mukkamalla SKR. Lymphoma. In: StatPearls. Treasure Island, FL: StatPearls Publishing; 2021 Accessed March 6, 2021 at: http://www.ncbi.nlm.nih.gov/books/NBK560826/
23 Camacho JC, Moreno CC, Harri PA, Aguirre DA, Torres WE, Mittal PK. Posttransplantation lymphoproliferative disease: proposed imaging classification. Radiographics 2014;34(07): 2025–2038
24 Strauss DC, Hayes AJ, Thomas JM. Retroperitoneal tumours: review of management. Ann R Coll Surg Engl 2011;93(04):275–280
25 Hoarau N, Slim K, Da Ines D. CT and MR imaging of retroperitoneal schwannoma. Diagn Interv Imaging 2013;94(11):1133–1139
26 Garrouche N, Ben Abdallah A, Arifa N, et al. Spectrum of gastrointestinal lesions of neurofibromatosis type 1: a pictorial review. Insights Imaging 2018;9(05):661–671
27 Johnson SA, Kumar A, Matasar MJ, Schöder H, Rademaker J. Imaging for staging and response assessment in lymphoma. Radiology 2015;276(02):323–338
28 Hussain MH, Iqbal Z, Mithani MS, Khan MN. Retroperitoneal ganglioneuroma in a patient presenting with vague abdominal pain. Cureus 2020;12(07):e9133
29 Ghoneim S, Shah A, Han K, Cai D, Sandhu D. Endoscopic management of ganglioneuroma in the stomach. ACG Case Rep J 2020;7 (05):e00382
30 Arab N, Alharbi A. Retroperitoneal ganglioneuroma (GN): case report in 14 years old boy. Int J Surg Case Rep 2019; 60:130–132
31 Koktener A, Kosehan D, Akin K, Bozer M. Incidentally found retroperitoneal ganglioneuroma in an adult. Indian J Surg 2015; 77(Suppl 1):3–5
32 Guan YB, Zhang WD, Zeng QS, Chen GQ, He JXCT. CT and MRI findings of thoracic ganglioneuroma. Br J Radiol 2012;85(1016): e365–e372
33 Decarolis B, Simon T, Krug B, et al. Treatment and outcome of ganglioneuroma and ganglioneuroblastoma intermixed. BMC Cancer 2016;16:542
34 Gill T, Adler K, Schrader A, Desai K, Wermers J, Beteselassie N. Extra-adrenal pheochromocytoma at the organ of Zuckerkandl: a case report and literature review. Radiol Case Rep 2017;12(02): 343–347
35 Sanyal R, Remer EM. Radiology of the retroperitoneum: case-based review. AJR Am J Roentgenol 2009;192(6, Suppl):S112-–S117, Quiz S118–S121)
36 Shen Y, Zhong Y, Wang H, et al. MR imaging features of benign retroperitoneal paragangliomas and schwannomas. BMC Neurol 2018;18(01):1
37 Roberts AS, Shetty AS, Mellnick VM, Pickhardt PJ, Bhalla S, Menias CO. Extramedullary haematopoiesis: radiological imaging features. Clin Radiol 2016;71(09):807–814
38 Caiafa RO, Vinuesa AS, Izquierdo RS, Brufau BP, Ayuso Colella JR, Molina CN. Retroperitoneal fibrosis: role of imaging in diagnosis and follow-up. Radiographics 2013;33(02):535–552
39 Surabhi VR, Menias C, Prasad SR, Patel AH, Nagar A, Dalrymple NC. Neoplastic and non-neoplastic proliferative disorders of the perirenal space: cross-sectional imaging findings. Radiographics 2008;28(04):1005–1017
40 Kumar P, Singh A, Gamanagatti S, Kumar S, Chandrashekhara SH. Imaging findings in Erdheim-Chester disease: what every radiologist needs to know. Pol J Radiol 2018;83:e54–e62

